

RESEARCH ARTICLE

10.1002/2016SW001465

Key Points:

- This is the first statistical comparison between data and magnetosphere models
- Global MHD models statistically perform worse during active time periods
- Including coupling to a ring current code statistically improves the MHD model

Correspondence to:

A. J. Ridley,
ridley@umich.edu

Citation:

Ridley, A. J., D. L. De Zeeuw, and L. Rastätter (2016), Rating global magnetosphere model simulations through statistical data-model comparisons, *Space Weather*, 14, 819–834, doi:10.1002/2016SW001465.

Received 7 JUL 2016

Accepted 23 SEP 2016

Accepted article online 30 SEP 2016

Published online 22 OCT 2016

Rating global magnetosphere model simulations through statistical data-model comparisons

A. J. Ridley¹, D. L. De Zeeuw¹, and L. Rastätter²

¹Climate and Space Sciences and Engineering, University of Michigan, Ann Arbor, Michigan, USA, ²Community Coordinated Modeling Center, Goddard Space Flight Center, Greenbelt, Maryland, USA

Abstract The Community Coordinated Modeling Center (CCMC) was created in 2000 to allow researchers to remotely run simulations and explore the results through online tools. Since that time, over 10,000 simulations have been conducted at CCMC through their runs-on-request service. Many of those simulations have been event studies using global magnetohydrodynamic (MHD) models of the magnetosphere. All of these simulations are available to the general public to explore and utilize. Many of these simulations have had virtual satellites flown through the model to extract the simulation results at the satellite location as a function of time. This study used 662 of these magnetospheric simulations, with a total of 2503 satellite traces, to statistically compare the magnetic field simulated by models to the satellite data. Ratings for each satellite trace were created by comparing the root-mean-square error of the trace with all of the other traces for the given satellite and magnetic field component. The 1–5 ratings, with 5 being the best quality run, are termed “stars.” From these star ratings, a few conclusions were made: (1) Simulations tend to have a lower rating for higher levels of activity; (2) there was a clear bias in the B_z component of the simulations at geosynchronous orbit, implying that the models were challenged in simulating the inner magnetospheric dynamics correctly; and (3) the highest performing model included a coupled ring current model, which was about 0.15 stars better on average than the same model without the ring current model coupling.

1. Introduction

In the mid-1980s, global magnetospheric models started to be created. These models allowed researchers to explore various aspects of the solar wind-magnetosphere-ionosphere system [e.g., Fedder and Lyon, 1987]. The Lyon-Fedder-Mobarry (LFM) magnetohydrodynamic (MHD) code [Fedder *et al.*, 1998; Lyon *et al.*, 2004] was one of the first global magnetosphere models. The LFM solves the MHD equations on a distorted spherical mesh in order to align the grid with the magnetic field as much as possible. This results in less numerical diffusion in the code in the inner magnetosphere, where currents are calculated for the ionospheric solver. The LFM has been coupled with a thermosphere-ionosphere model [Wiltberger *et al.*, 2004; Wang *et al.*, 2004] and the Rice Convection Model [Toffoletto *et al.*, 2004]. It is available at the Community Coordinated Modeling Center (CCMC) for runs-on-request, as will be described later.

The Open Geospace General Circulation Model (OpenGGCM) is also an MHD-based code that has been used in many scientific investigations [Raeder *et al.*, 1996, 1997, 1998, 2001a]. The OpenGGCM uses a stretched Cartesian grid, concentrating high-resolution grids anywhere in the magnetosphere. The OpenGGCM has been coupled to a thermosphere-ionosphere model [Raeder *et al.*, 2001b] and is also available at CCMC.

Robert Winglee’s code solves the multifluid MHD equations [Winglee, 1995, 1998]. This code was used to explore the problem of ion outflow earlier than any other global code, since it resolved oxygen, hydrogen, and helium ions in the magnetosphere before other global models. The code is not available at the CCMC at the time of this writing. The Mission Research Corporation (MRC) MHD code is similar to Winglee’s code but goes a step further—it models the magnetosphere and ionosphere as one system [White *et al.*, 1998]. The MRC code is also not available at the CCMC. The MHD code described by Tanaka [1995] is also a global magnetosphere-ionosphere code that is more widely used outside of the United States and is not available at the CCMC.

The Block Adaptive Tree Solar wind Roe-type Upwind Scheme (BATSUS) MHD code [Powell *et al.*, 1999; Gombosi *et al.*, 2001, 2004] also solves for the global magnetosphere. A relatively simple yet effective

block-based adaptive mesh refinement (AMR) technique was developed and is used in conjunction with a finite-volume scheme [Stout *et al.*, 1997] to solve the MHD equations. At the CCMC, a variety of grids are available, all of which are static in time but can vary significantly throughout the domain. BATSRUS has been coupled to a variety of inner magnetosphere models [e.g., De Zeeuw *et al.*, 2004; Zhang *et al.*, 2007; Glocer *et al.*, 2009; Zaharia *et al.*, 2010]. Multispecies (multiple-continuity and single-momentum equations) and multifluid (multiple-continuity and multiple-momentum equations) versions of BATSRUS were developed and have been used for scientific studies [e.g., Welling and Ridley, 2010b; Welling *et al.*, 2011; Welling and Zaharia, 2012; Welling and Liemohn, 2014; Yu and Ridley, 2013a, 2013b]. Different versions of BATSRUS are available for runs-on-request at CCMC, as it will be described below.

The Grand Unified Magnetosphere-Ionosphere Coupling Simulation (GUMICS) MHD code is similar to BATSRUS in that it uses an adaptive grid architecture and similar solvers [e.g., Janhunen, 1996; Palmroth *et al.*, 2001, 2005]. It is different from BATSRUS in that it does not use blocks but allows each cell to be split into eight subcells. GUMICS has a three-dimensional ionosphere in order to resolve the ionospheric densities and conductivities [Palmroth *et al.*, 2004, 2006]. It is also available for runs-on-request at CCMC.

A wide variety of studies have been conducted to validate global MHD models of the magnetosphere. For example, Ridley *et al.* [2002] explored the ionospheric drift velocities predicted by the BATSRUS magnetospheric model coupled to an ionospheric potential solver. Raeder *et al.* [1998] explored how well an MHD code matched boundaries in the ionosphere, such as the low-latitude boundary layer. Raeder *et al.* [1997] investigated how the MHD code compared against measurements by the Geotail satellite.

The studies by Wang *et al.* [2008], Korth *et al.* [2011], and Kleiber *et al.* [2016] compared field-aligned currents produced by global MHD codes projected to the ionosphere to different satellite measurements. Raeder *et al.* [2001a], Ridley *et al.* [2001], Yu *et al.* [2010, 2008], and Pulkkinen *et al.* [2010, 2011] all validated MHD codes by comparing ground-based magnetometer data to simulation results by computing the magnetic perturbation that would be registered on the ground using different current systems in the ionosphere, magnetosphere, and the gap region between the two. Global MHD codes have also been compared to geosynchronous satellite measurements of magnetic fields, as shown by Taktakishvili *et al.* [2007], Welling and Ridley [2010a], and Honkonen *et al.* [2013].

While the majority of the validation studies described above highlight how one code compares against a single type of data, some of them have compared different models against the same type of data or different models against different data [Pulkkinen *et al.*, 2010, 2011; Honkonen *et al.*, 2013]. Because MHD models have historically needed significant computational resources to run, the comparisons have been quite limited, focusing on a small number of events. Recently, the Community Coordinated Modeling Center (CCMC) has led validation studies in which different models were run for the same time periods in order to compare how well they performed against each other. For example, Pulkkinen *et al.* [2011] compared different model results of ground-based magnetic field perturbations to magnetometer measurements to determine the capabilities of the different models. Rastätter *et al.* [2016] compared different models against DMSP poynting flux in the ionosphere. Rastätter *et al.* [2013] focused on the ability of many different models in many different configurations to reproduce *Dst* from four different events. The assessment was also completed with a variety of different metrics. They found that MHD models that are coupled to an inner magnetospheric ring current model performed better during storms than other MHD models. Both Pulkkinen *et al.* [2010] and Rastätter *et al.* [2011] included geosynchronous data in a similar evaluation.

Statistical comparisons between models and data have been attempted as well. Gordeev *et al.* [2015] compared different models by running nominal conditions and comparing to statistical models. The goal of that study was to determine whether the different models reproduced key parameters within the magnetosphere, such as the size. They concluded that no model was better than any other model. Zhang *et al.* [2011] compared a 2 month simulation of the LFM model to a number of ionospheric electrodynamic quantities. This was one of the first long-term simulations of a global MHD model.

Even with these types of studies, a very small number of simulations were conducted to complete the comparisons. In this study, statistical comparisons are made between global MHD simulation results and satellite-based magnetic field measurements. Specifically, the general ability of global models to simulate

active versus quiet conditions is explored. In addition, the different models are statistically compared to each other to determine whether there are models that are statistically better at modeling the magnetosphere. Finally, statistical model biases are explored.

2. Methodology

The CCMC has a program in which a user can request simulations of the geospace environment by specifying a domain to simulate, the model to use, and a time period to run. The simulation is then conducted at CCMC, and the model results are made available through a web interface to allow the user (and the entire community) to visualize the simulation results. Further, CCMC has traced virtual satellites through many of the simulation results, allowing direct comparisons between the model results and the satellite data. As of December 2014, when the study obtained data from the Virtual Model Repository (VMR), there were 662 magnetospheric simulations at CCMC that had such traces through them. The satellites that were considered in this study were GOES 8, GOES 9, GOES 10, GOES 11, GOES 12, Geotail, THEMIS A, THEMIS B, THEMIS C, THEMIS D, THEMIS E, and Cluster 1. A total of 2503 satellite tracks were used.

At the VMR, the CCMC-produced simulation results along the satellite trajectory, along with all of the observational data, were downloaded and compared. Figures 1 and 2 show examples of comparisons between simulations conducted at CCMC and data from GOES 11 and GOES 12, respectively. Four simulations are shown for the 14–15 December 2006 storm. These simulations were carried out with (a) OpenGGCM [Raeder, 2003], (b) BATSRUS [Powell *et al.*, 1999], (c) LFM [Lyon *et al.*, 2004] and (d) GUMICS [Janhunen, 1996]. There are some clear differences between the simulation results and the data. For example, the OpenGGCM results had large perturbations in the second half of the time period, while the data do not show these perturbations. On the other hand, the OpenGGCM matched the B_z component in the middle of the time period better than the other models. BATSRUS captured the overall structure quite well but missed a large amount of the variability in the data. For GOES 12, BATSRUS underestimated the magnetospheric response in all three components in the middle of the time period. LFM also captured the overall structure, and some of the variability, but seemed to have too much variability at times. GUMICS appeared to show some semidiurnal variations during the time period in the B_x and B_y components and looked remarkably like the BATSRUS model results in the B_z component.

While four simulations are shown for this storm case, there were actually 15 simulations at CCMC of this storm. Each of these simulations can be compared in exactly the same manner as shown in Figures 1 and 2. Indeed, all of the 662 magnetospheric simulations that have satellite traces through them were compared in this way. For each of the simulations and each of the different satellites and magnetic field components, the average difference, root-mean-square (RMS) error, and normalized RMS error (i.e., RMS error divided by mean of the data multiplied by 100%) between the simulation result and the observational data were computed and saved. These average differences and RMS errors were then explored to gain a better understanding of how each simulation compared against all of the other simulations that were conducted.

Figures 3 and 4 show statistical histograms of the comparisons between the simulation results and the GOES 11 and GOES 12 satellite measurements of the magnetic field, respectively. For both satellites (and all the other geosynchronous satellites including GOES 8, GOES 9, and GOES 10), the median error in B_x and B_y were close to 0, with a roughly symmetric distribution. For B_z , the distribution had a clear bias in the positive direction, with the distribution roughly symmetric around this positively biased value. For the other satellites, the three magnetic field components were roughly symmetric around zero error (not shown). This is quantified in Table 2.

In Figures 3 (middle column) and 4 (middle column), the root-mean-square error distributions are shown from the simulations. B_x and B_y show distributions that have peaks below 5 nT and taper slowly off from there. The B_z distributions peak at higher values (close to 10–15 nT), consistent with the median errors. It is asserted that a simulation that had, for example, an error in B_x of less than 1 nT simulated B_x better than a simulation that had an error in B_x of 30 nT. The idea of “better” has been quantified by breaking the RMS errors into five distinct regions, assigning them ratings of 5 (best), with very low RMS errors, down to 1 (worst), with very high RMS errors. The demarcations between the five different ratings are indicated by the vertical lines in the

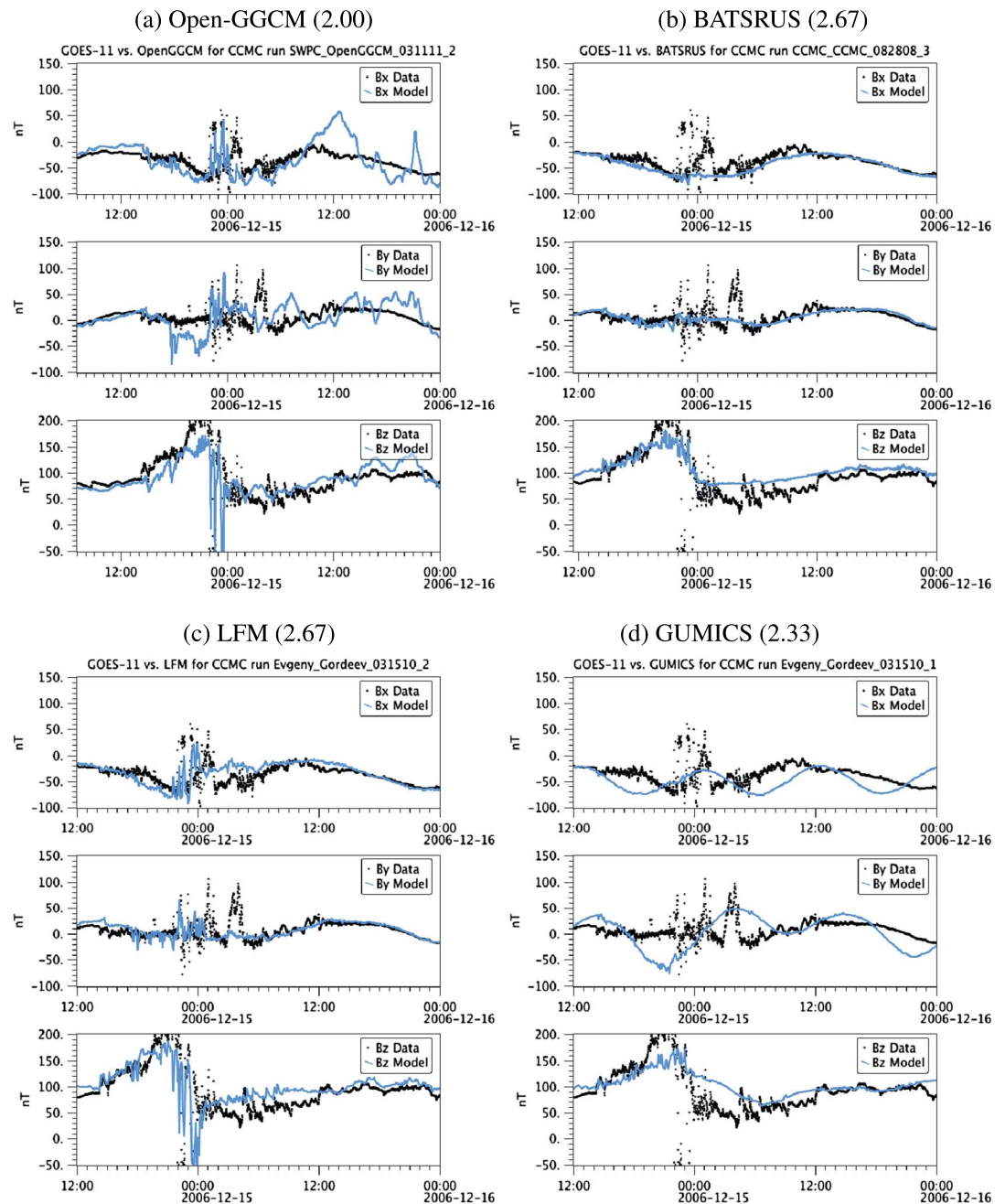


Figure 1. Comparisons between model results and GOES 11 satellite measurements of the magnetic field during 14 December 2006.

plots in Figures 3 (middle column) and 4 (middle column). The placement of these demarcations are described completely below. The plots in Figures 3 (right column) and 4 (right column) are distributions of errors in normalized RMS error, where the normalization is done with the mean of the measured data.

From zero RMS (or nRMS) error to the blue line were all of the runs with a rating of 5 for that particular satellite and component of the magnetic field. RMS (or nRMS) errors between the blue to the yellow lines were assigned a rating of 4. Yellow to orange indicated a rating of 3, etc. Originally, the demarcations were determined by taking the mean and standard deviation and linearly combining these in a way to give roughly normal distributions for the ratings, but this did not work well for some satellites. For example, the GOES 12

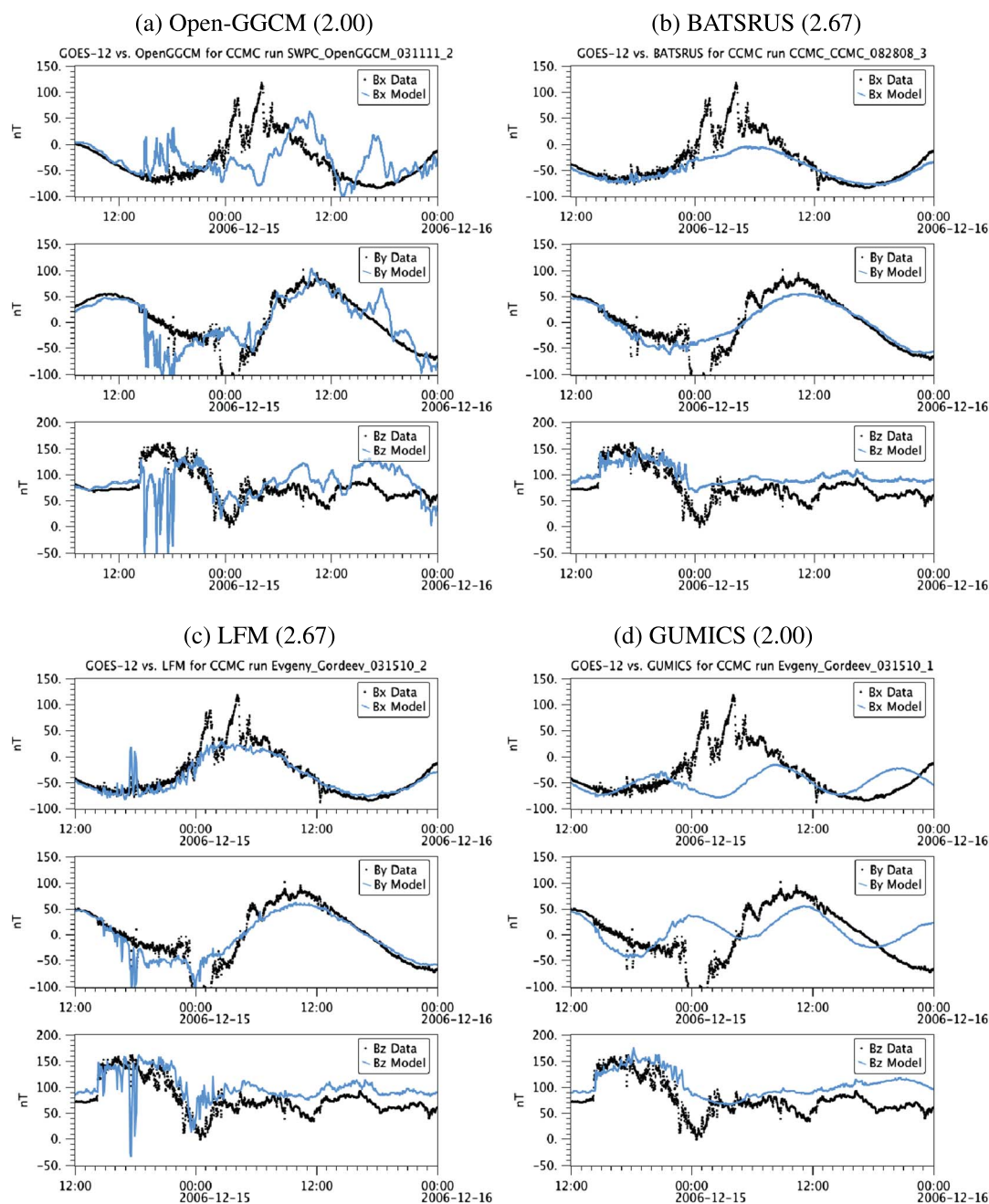


Figure 2. Comparisons between model results and GOES 12 satellite measurements of the magnetic field during 14 December 2006.

RMS error distributions had extremely long tails. By choosing linear combination coefficients of the mean and standard deviation that worked well for other satellites, the GOES 12 rating distribution was skewed toward low ratings.

For this study, the rating distributions, as described by the vertical lines in Figures 3 and 4, were determined by first sorting all of the RMS errors for the particular satellite and magnetic field component, and then determining the values that were 7.7%, 30.8%, 69.2%, and 92.3% of the way through the list. These percentages produced distributions that were roughly 1, 3, 5, 3, and 1 in population for the 5, 4, 3, 2, and 1 rankings, respectively, in most individual satellite magnetic field component comparisons. The same ranking scheme was used

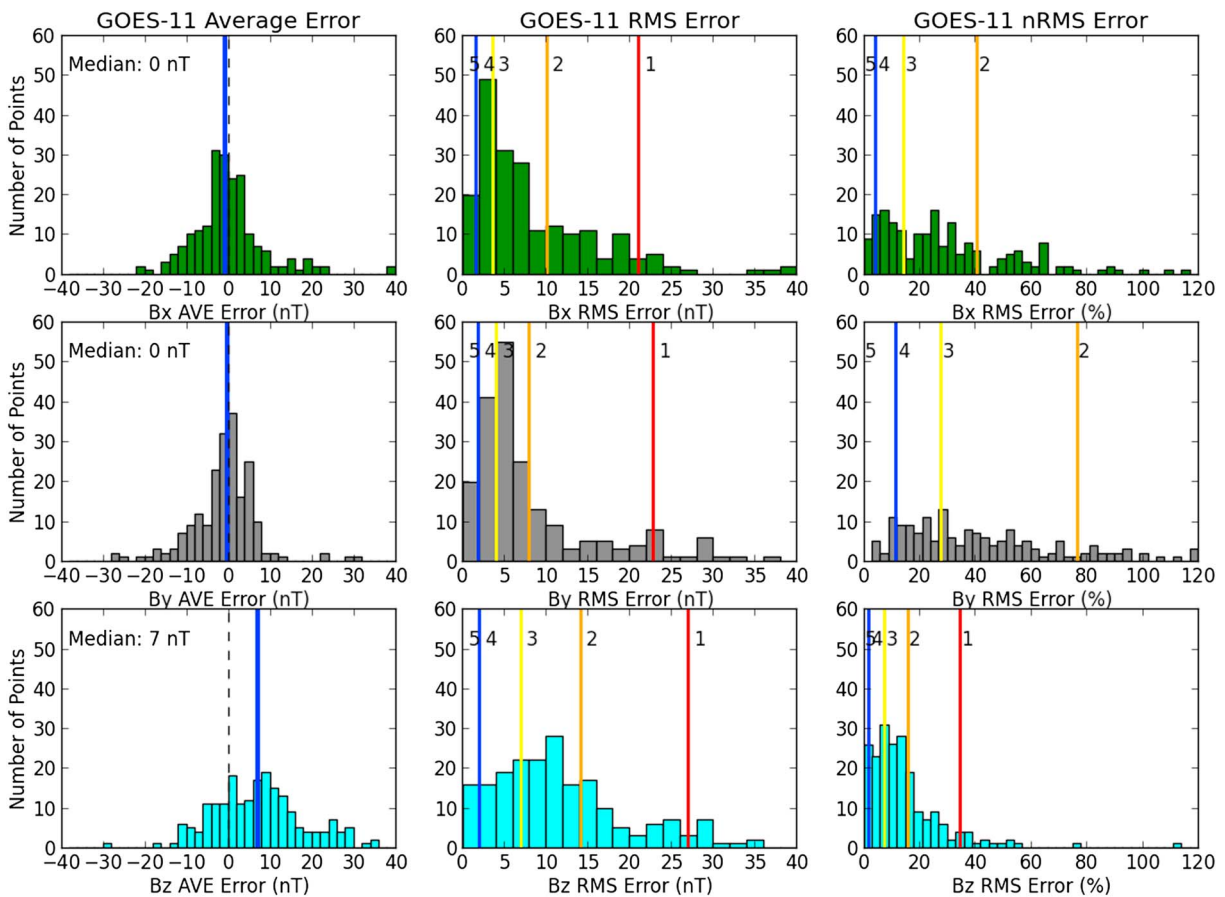


Figure 3. Distributions of (left column) difference error, (middle column) root-mean-square error, and (right column) normalized RMS error for (top row) B_x , (middle row) B_y , and (bottom row) B_z for the GOES 11 satellite.

for the normalized RMS errors. The rankings for both RMS and nRMS are indicated by the blue, yellow, orange, and red lines, respectively, in Figures 3 and 4. The RMS and nRMS ratings were kept separate from each other in order to determine whether conclusions made with one type of assessment are consistent with another type of assessment.

The 1–5 run ratings qualities are termed “stars,” since they are roughly equivalent to a user rating of the simulation. Each of the three magnetic field components for a simulation-satellite combination was given a star rating (from 1 to 5 as described above). So for example, if a simulation run had the same 10 nT RMS error in all three of GOES 12 B_x , B_y , and B_z magnetic field components, the ratings for the three components would be 3, 3, and 4, respectively. These three star ratings would then be averaged together to give a star rating for the simulation-satellite combination. In the example above, the average for the GOES 12-model comparison would be 3.33. Most of the time each run had multiple satellites traced through the results, such that the star ratings for each of these satellite comparisons could be averaged to provide an overall star rating for the particular simulation. Given that there were 662 simulations and 2503 satellite traces, an average of 3.78 satellite traces existed for each simulation.

Figures 5 and 6 show the distributions of the star ratings for all of the satellite-simulation combinations included in this study, sorted by satellite. The top plots (blue histograms) show the histograms of the RMS star ratings, while the bottom plots (red histograms) show the histograms of the nRMS star ratings. Most of the histogram shows what one would expect—the most probable value is close to the mean value of around 3, with very few simulations receiving very high or very low star ratings. In Figure 5, most of the GOES satellite results have somewhat skewed distributions, with a second peak a bit above the mean value, around 3.67 stars. GOES 9 does not have very many data points, so it is hard to determine whether this is significant at all. The GOES 10, GOES 11, and GOES 12 satellites have hundreds of comparisons, so the skewed distribution is

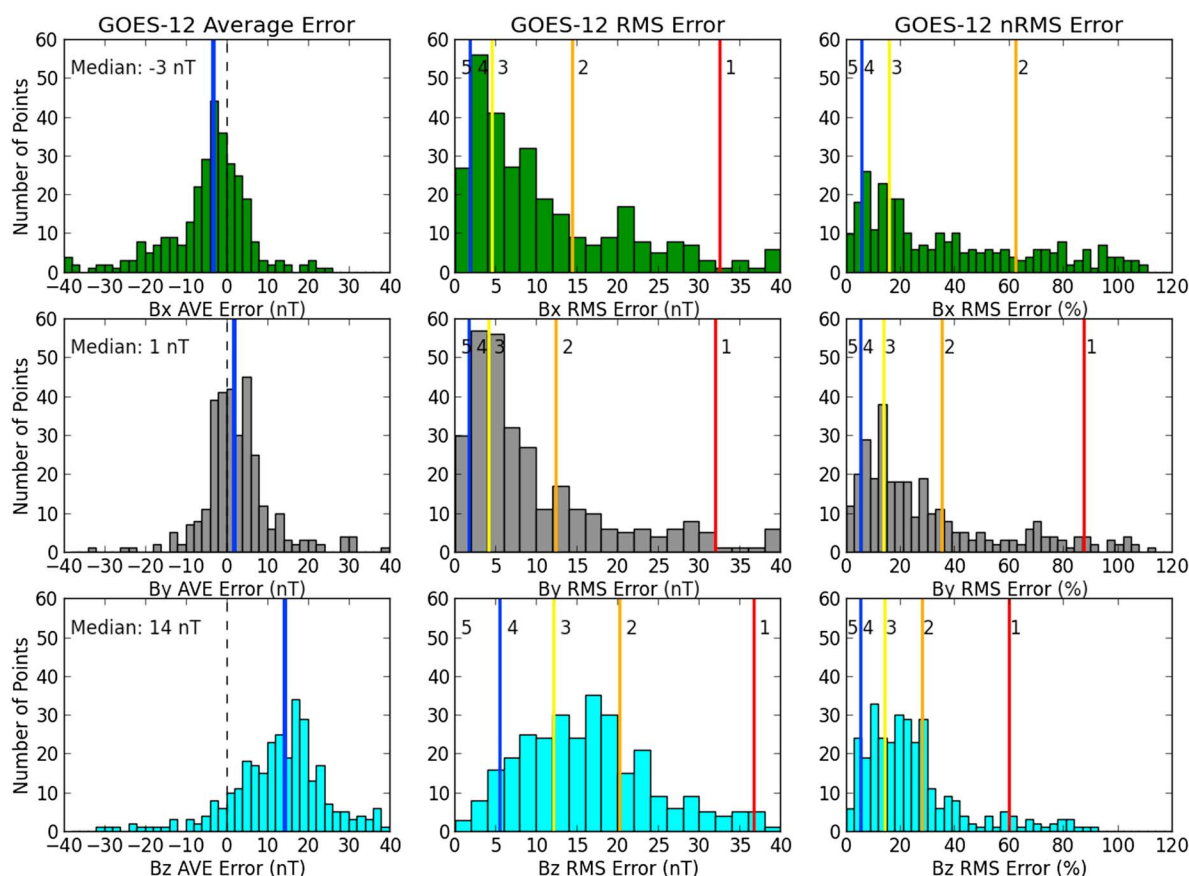


Figure 4. Distributions of (left column) difference error, (middle column) root-mean-square error, and (right column) normalized RMS error for (top row) B_x , (middle row) B_y , and (bottom row) B_z for the GOES 12 satellite.

possibly meaningful, when compared to other satellites, such as Geotail. While exploring why this might be the case is beyond the scope of the current study, it is noteworthy that these types of possible differences in data sets can be observed in this type of statistical study.

Figure 6 shows the distributions of the star ratings for the five THEMIS satellites and one of the Cluster satellites. The other Cluster satellites were not included since the spacing between the Cluster satellites was typically on the same magnitude or closer than the grid spacing in most of the simulation results. This means that the RMS errors between each of the Cluster satellites and the simulation results would all be very similar to each other. There are significantly less data points for the THEMIS and Cluster satellites, since they have not been in space for as long as some of the GOES or Geotail satellites have been. The distributions for most of the satellites look roughly normal, with peaks close to the median value, which are all close to three stars. There are not enough Cluster data points to determine whether the distribution is skewed.

3. Results

While there are many different types of analyses that can be conducted on the simulations that are presented in this study, three are focused on here: (1) the relationship between the star rating and the activity level, as indicated by the disturbance storm time (Dst) index, that was occurring during the time, (2) the mean star rating for individual models, and (3) the biases that can exist within the models that point to possibly missing physics.

Figure 7 shows the statistical relationship between the minimum Dst that occurred during the simulation time period and the star rating of that simulation for each of the simulations included in this study (top right). The vast majority of the simulations were conducted for nonstorm time periods, while only a small number covered superstorm periods. Examining the lower figure, it can be seen that there were multiple simulations

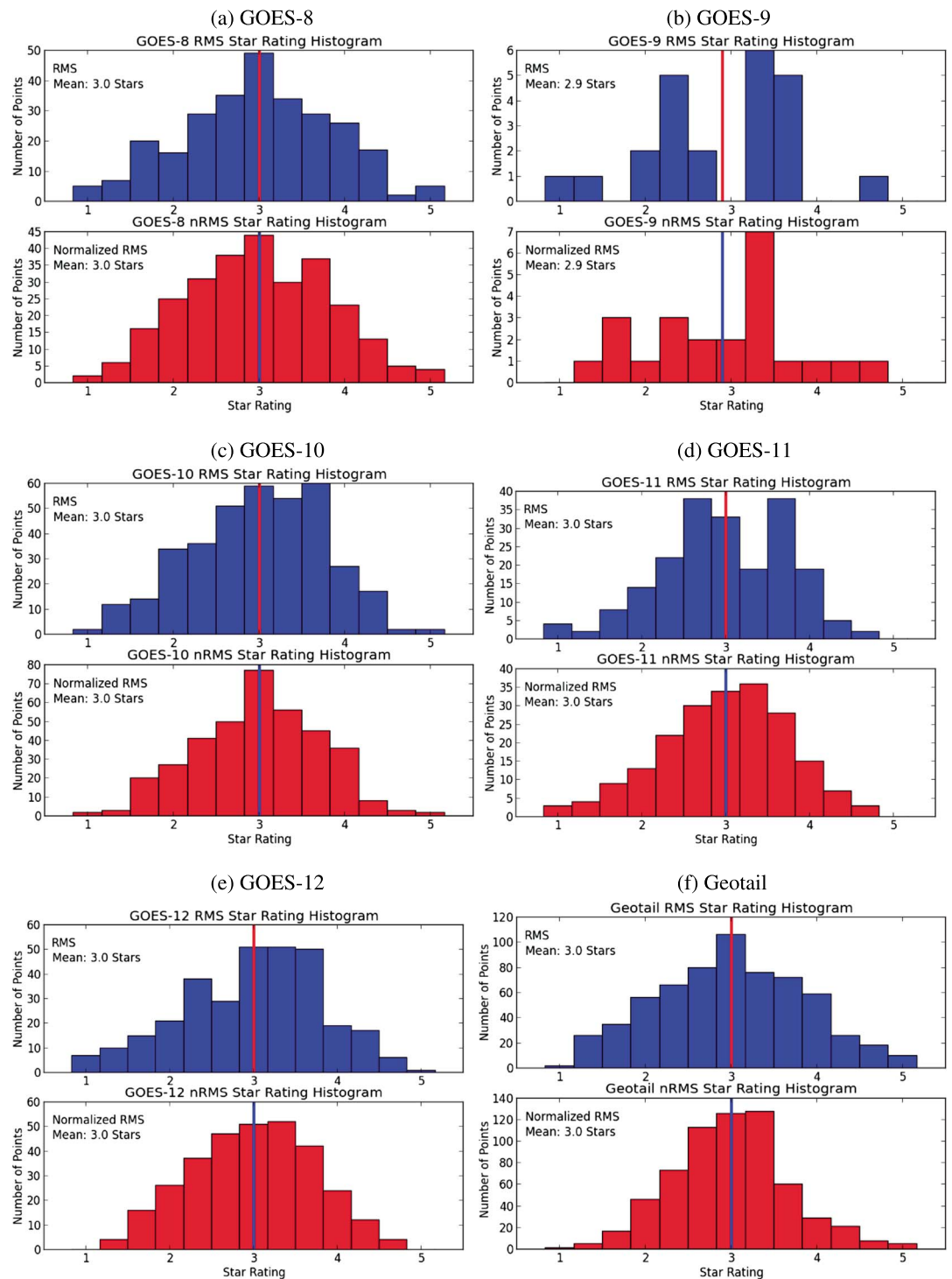


Figure 5. Star ratings for data-model comparisons between (a) GOES 8, (b) GOES 9, (c) GOES 10, (d) GOES 11, (e) GOES 12 and (f) Geotail. The mean star rating is indicated in each plot. The blue distributions show the RMS star ratings, while the red distributions show the nRMS star ratings.

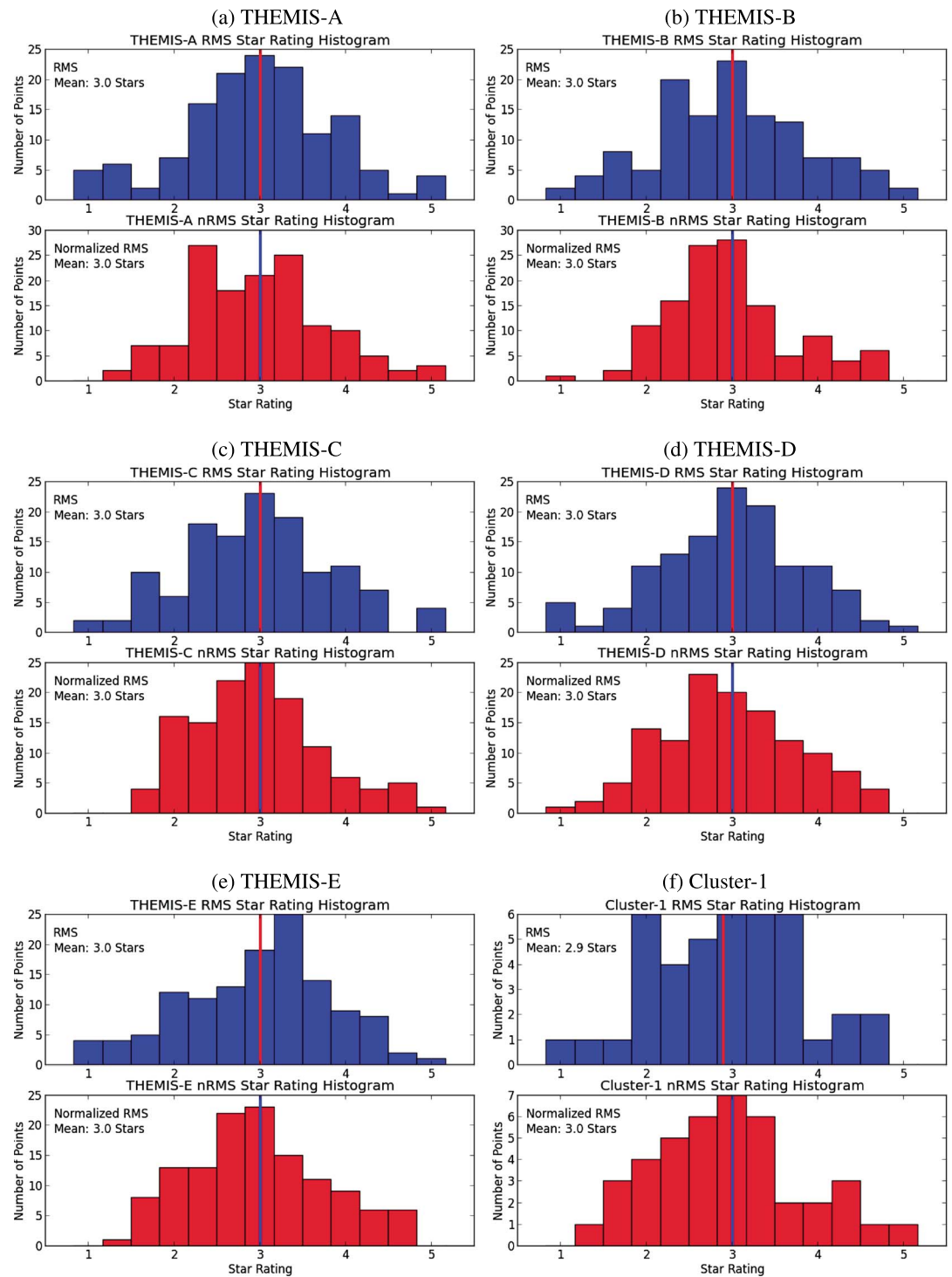


Figure 6. Star ratings for data-model comparisons between (a) THEMIS A, (b) THEMIS B, (c) THEMIS C, (d) THEMIS D, (e) THEMIS E, and (f) Cluster 1. The mean star rating is indicated in each plot. The blue distributions show the RMS star ratings, while the red distributions show the nRMS star ratings.

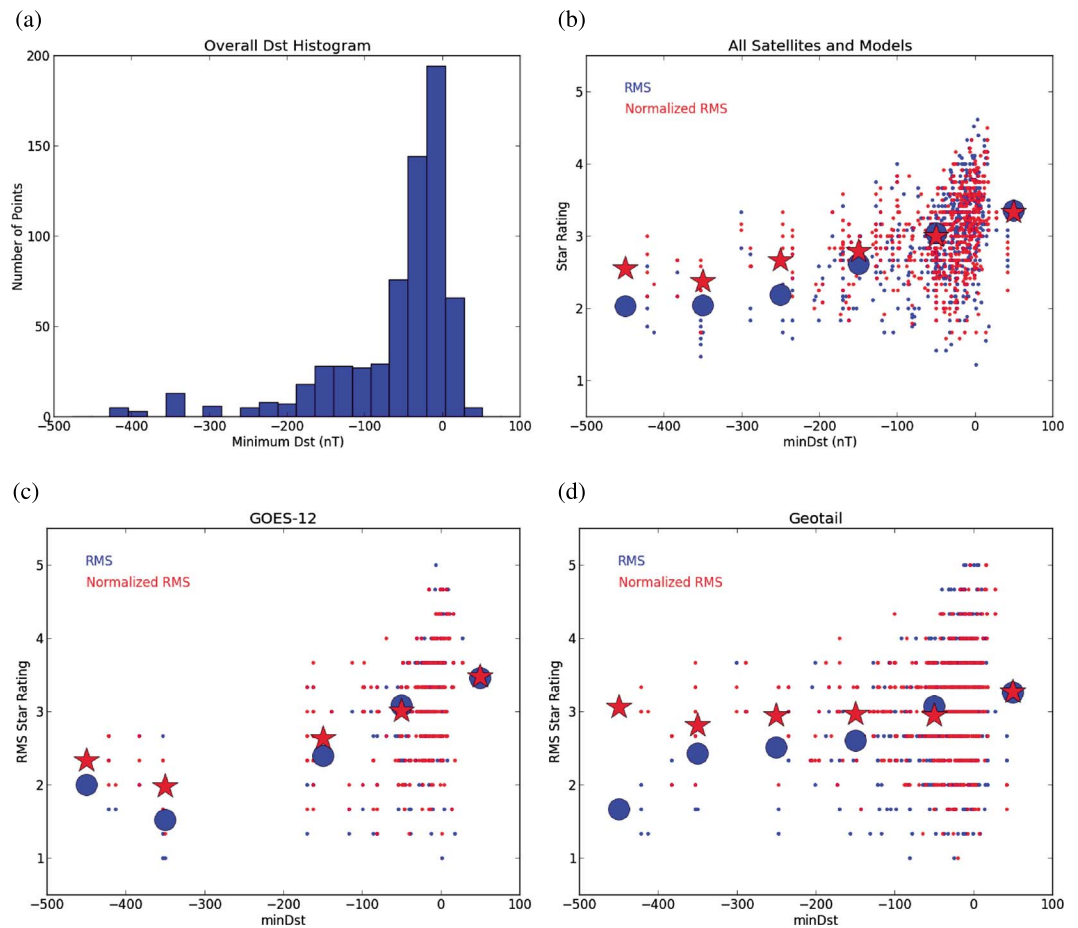


Figure 7. (a) A histogram showing the minimum Dst during all of the events that were included in this study. (b) Star rating of each of the simulations as a function of the minimum Dst during simulation time period. The blue dots indicate RMS star ratings, while the red dots indicate nRMS star ratings. The large symbols indicate the average star ratings in bins of 100 nT, centered on the symbol. The relationship between Dst and star rating for (c) GOES 12 and (d) Geotail.

with the exact same Dst value but different star values. These were simulations of the same event but using different models, different grids, or different drivers. As was described by Ridley *et al.* [2010], running the same model with different numerical schemes or grids can provide different results and therefore different qualities of simulation. Running the same event with different models can accentuate this, since the models may solve the MHD equations in completely different ways. This is observed in Figures 3 and 4.

The general trend in Figure 7b is that runs with higher levels of activity (i.e., more negative Dst) tend to have lower star ratings. At lower levels of activity (i.e., Dst near 0), the star ratings tend to be higher, although there is a huge amount of variability in run quality at lower activity levels. This trend appears to mean that global MHD codes consistently have a harder time simulating large storms but can often simulate quiet time periods very well. There are a couple of reasons why this might be the case.

First, the perturbations in the magnetic field away from a simple dipole are significantly larger during a storm than during a quiet time period, so if there is any error, it has the possibility of being much larger than during a quiet time. For example, if the code put the pressure increase from the ring current buildup in a slightly incorrect location during a storm, resulting in the current distribution being shifted by a few degrees, then the difference in the magnetic perturbations may be quite large. On the other hand, during a quiet time, when there are no large current systems, a slight shift of the pressure in the magnetosphere will not result in large differences in the magnetic perturbations, since the field would still be dominated by the dipolar background. The normalized RMS ratings back this idea up: in the largest storm events, the red dots (nRMS stars) are consistently above the blue dots (RMS stars). While the general trend of having worse results during major storms still exists, the trend appears to be weaker with the normalized RMS.

Second, the majority of the simulations that were included in this study were with global magnetospheric MHD models that do not include the physics of the ring current. This means that these models were not really expected to simulate storm times accurately, since the ring current dynamics dominate the inner magnetosphere during storm events. This will be discussed in more detail below, when individual models are compared.

The conclusion that the skewing of the distribution toward worse results as the activity level increased was due to the inner magnetospheric dynamics can be further explored by comparing two satellites: one that was in the inner magnetosphere (GOES 12, Figure 7c) and one that was not (Geotail, Figure 7d). The GOES 12 data show a strong dependence on Dst in both the RMS and nRMS results, with simulations of strong storms having an average star rating of one to two stars below the quiet times. Geotail, on the other hand, has very little dependence on activity level, especially in the normalized RMS, where the values are close to three stars, independent of activity level. In the RMS star values, there is a small decrease for moderate storms, but it is not as strong as the decrease in GOES 12. For the strongest storms (Dst between -400 and -500 nT), the statistics are very low for both the Geotail and GOES 12 data.

These results are consistent with *Rastätter et al.* [2013], who compared the simulated Dst from many different MHD models to the measured Dst . They showed that models that included coupling to inner magnetosphere models typically had better prediction efficiencies. The results presented here show that this tendency is also true if comparing to inner magnetospheric magnetic field measurements. It also expands the *Rastätter et al.* [2013] study from four events to several hundred.

Figure 8 shows distributions of star ratings for individual models that are included in CCMC runs-on-request. While there are more variations of individual models in the database, the models have been grouped into five categories:

1. *BATSRUS*. There have been many different versions of BATSRUS at CCMC. Each of these versions had been coupled to an ionospheric electrodynamics solver, described by *Ridley et al.* [2004] and *Ridley and Liemohn* [2002]. The specific versions that were included in this list were v6.07, v7.42, v7.73, v8.00, and v8.01. Some of these versions were significant upgrades to the model, but in the standard runs at CCMC, very few of the new features were implemented, so the versions were run in ways that were very similar to each other. In addition, some of the runs were tagged as being part of the Space Weather Modeling Framework (SWMF), which is described by *Tóth et al.* [2005]. SWMF, as run at the CCMC, was similar to the older BATSRUS versions, which included only coupling to the ionospheric electrodynamics.
2. *BATSRUS with RCM*. In this version of the code, the BATSRUS model was coupled to the Rice Convection Model (RCM), as described by *De Zeeuw et al.* [2004], and the ionospheric electrodynamics code using the SWMF. The inner magnetospheric dynamics were described with the RCM, so in theory, storm time dynamics could be captured with more accuracy with this coupled model. The specific versions of BATSRUS that were run coupled to RCM at CCMC were v7.73, v8.01, and v20101108. Updated versions of this model, which include coupling to the Comprehensive Ring Current Model [e.g., *Fok et al.*, 2008], and a newer version of the RCM, are currently available at CCMC but were not included in this study.
3. *GUMICS*. The GUMICS MHD code was similar to BATSRUS in that it used an adaptive grid architecture [e.g., *Janhunen*, 1996] and was coupled to an ionospheric electrodynamics solver [e.g., *Palmroth et al.*, 2005]. The specific versions of GUMICS that were run at CCMC included 4-HC-1.11 and 4-HC-20140326.
4. *LFM*. The LFM MHD code was fully described by *Lyon et al.* [2004]. The specific versions of LFM included here include 1, 1.04, 1.05, LTR-2_1_1, LTR-2_1_4, LTR-2_1_5, and LTR-2_2_0. These versions were coupled to an ionospheric electrodynamics solver, described by *Merkin and Lyon* [2010], and a coupled ionosphere-thermosphere model, as described by *Wang et al.* [2004].
5. *OpenGGCM*. The OpenGGCM was described in many papers, including (for example) *Raeder et al.* [1996, 1997, 2001b, 2003]. This code was coupled to an ionospheric electrodynamics solver and a global ionosphere-thermosphere model [Fuller-Rowell and Rees, 1983]. The specific versions included at the CCMC and in this study were 2.1-1, 3.0, 3.1, and 4.0.

Figure 8 shows that BATSRUS was the most used model at the time of this study (286 simulations), with BATSRUS coupled to the RCM being the second most used (165 simulations) and the OpenGGCM having the third most simulations (151). GUMICS had been used the least of any of the models (12 simulations). LFM had a total of 49 simulations. Because there were differences in the numbers of samples in each distribution, and since the distributions all looked slightly different, a Kolmogorov-Smirnov test was used to determine the probability

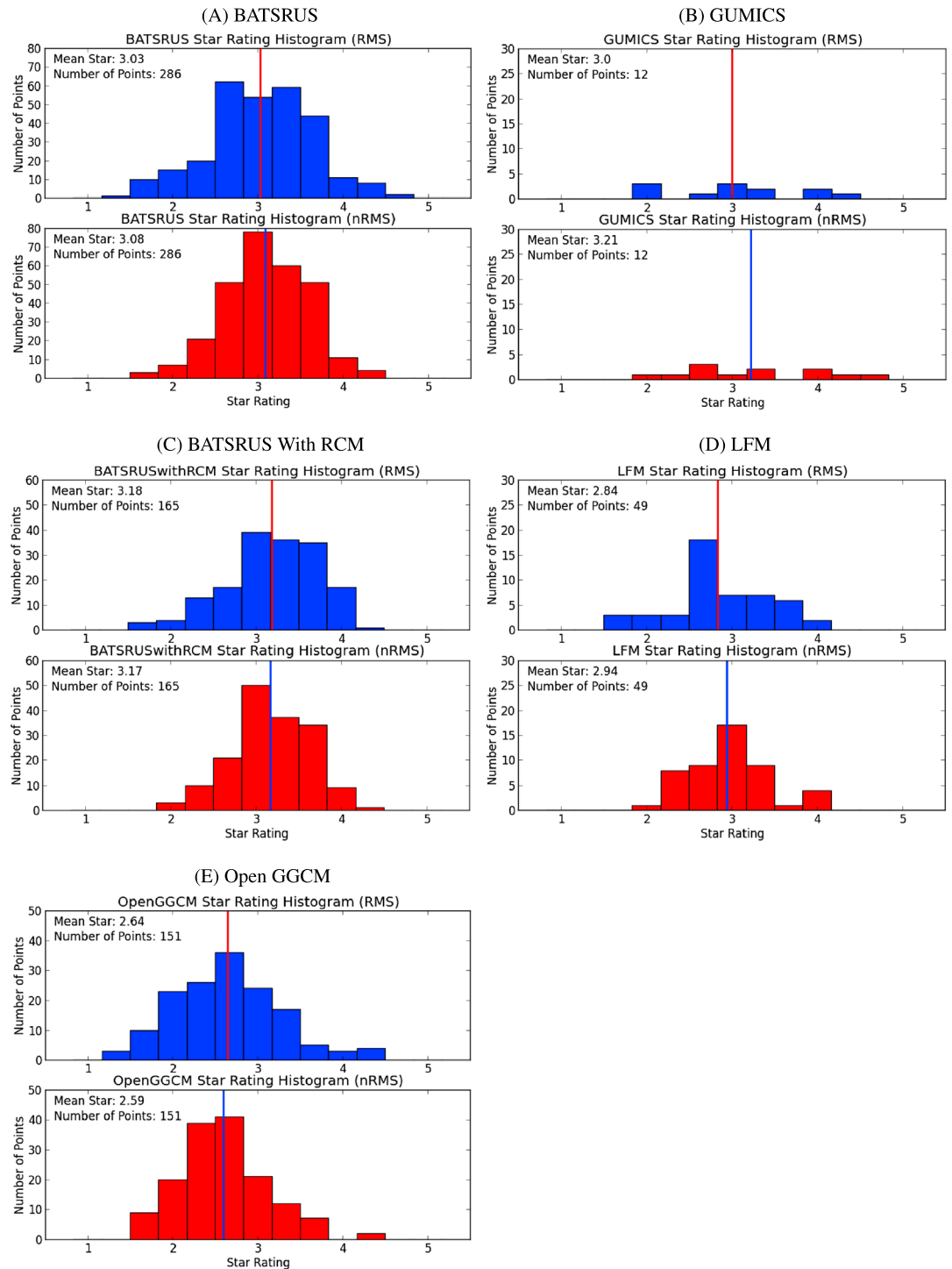


Figure 8. Overall star ratings for simulations broken down by individual models. (A) BATSURUS, (B) GUMICS, (C) BATSURUS coupled to the RCM, (D) LFM, and (E) OpenGGCM. More detail is provided in the text.

that the distributions were the same. Table 1 shows the results of those tests. If the probability is low, it indicates that the distributions were most likely different from each other, and that the differences in star ratings for the different models were statistically significant. If the probability was high, it implies that the distributions were similar (or that there was not enough data to determine whether the distributions were different) and that the differences in star rating were not statistically significant. Table 1 indicates that (a) there were not enough data to determine if GUMICS was statistically different than any of the other models, meaning

Table 1. Kolmogorov-Smirnov Statistical Results Showing the Probability That the Two Distributions Are From the Same Sampling Pool

Model	B/RCM		OpenGGCM		LFM		GUMICS	
	RMS	nRMS	RMS	nRMS	RMS	nRMS	RMS	nRMS
BATSRUS	0%	11%	0%	0%	3%	11%	83%	27%
B/RCM			0%	0%	0%	0%	39%	32%
OpenGGCM					3%	0%	18%	3%
LFM							69%	30%

that any differences in star rating are mostly meaningless; (b) there was a small chance that LFM was similar to BATSRUS and a very small chance that it was similar to OpenGGCM but almost no chance that it was similar to BATSRUS with RCM, meaning that star rating comparisons between LFM and BATSRUS with RCM are valid, but comparisons with other models are questionable; (c) there was a small chance that BATSRUS and BATSRUS with RCM were chosen from the same distribution with the normalized RMS but not with the RMS; and (d) there was almost no chance that OpenGGCM was similar to BATSRUS or BATSRUS with RCM, implying that comparisons between the star ratings for these models is valid. As more simulations are conducted at CCMC with LFM and GUMICS, it will be easier to determine the actual distributions to explore how the models statistically compare to the other models.

All of the models have very similar star ratings, with BATSRUS with RCM having the highest at 3.18 (3.17 nRMS) and OpenGGCM having the lowest at 2.64 (2.59 nRMS), for a mean spread of about 0.54 stars. BATSRUS, GUMICS, and LFM have similar average star ratings with BATSRUS having a rating of 3.03 (3.08 nRMS), LFM having a star rating of 2.84 (2.94 nRMS), and GUMICS having a rating of 3.0 (3.21 nRMS). These results indicate that including an inner magnetosphere model makes a small, but statistically significant, difference to the model results. While these results might be interesting, they most likely do not indicate whether a given simulation will be better or worse with a given model, since there is so much spread around the mean rating of each model. In addition, other factors, such as model resolution, may play a large role in determining the star rating. These factors are not accounted for here but could be explored in further studies.

Table 2 shows the average errors for each of the three components of the magnetic field for each of the satellites. The mean values for the B_x and B_y components for the GOES geosynchronous satellites were near 0, while the B_z component had a strong positive value. This implies that the magnetic field in the majority of the model runs was too dipolar, as would be expected if the tail current within the simulations was too weak. For each of the other satellites that were not geosynchronous (Geotail, THEMIS X, and Cluster 1), the average of B_z was close to 0, indicating that the bias does not exist in the outer magnetosphere or at least away from geosynchronous orbit. With more analysis, this bias can be investigated much further, exploring which models had more bias, the local time dependence of the bias, and whether including a ring current model

Table 2. Satellites and Median Errors Associated With Each Component of the Magnetic Field

Satellite	Traces	B_x	B_y	B_z
GOES 8	274	-1 nT	0 nT	13 nT
GOES 9	23	0 nT	1 nT	10 nT
GOES 10	370	-1 nT	0 nT	18 nT
GOES 11	204	-1 nT	0 nT	6 nT
GOES 12	315	-3 nT	2 nT	13 nT
Geotail	632	0 nT	0 nT	-1 nT
THEMIS A	138	1 nT	0 nT	0 nT
THEMIS B	124	0 nT	0 nT	0 nT
THEMIS C	128	0 nT	0 nT	0 nT
THEMIS D	127	1 nT	0 nT	2 nT
THEMIS E	127	0 nT	1 nT	0 nT
Cluster 1	41	-1 nT	0 nT	-1 nT

helped to reduce the bias. This analysis is beyond the scope of the current study, which is simply introducing the statistical analysis that can be done with these model results.

4. Summary

This study used 662 magnetospheric simulations conducted at NASA's Community Coordinated Modeling Center (CCMC) that were carried out for a variety of users within the community over the last 14 years. Satellite trajectories were traced through each of these simulations to provide the magnetic field along the paths allowing direct comparisons between the satellite data and the simulation results. The root-mean-square (RMS) and normalized RMS error for each component of the magnetic field measured by each satellite were sorted, and four demarcation lines were created to separate the results into five bins, ranked from 1 (worst RMS or nRMS results) to 5 (best RMS or nRMS results). The demarcation lines were chosen such that the distribution of events would be 1, 3, 5, 3, and 1. The 1–5 ratings are termed “stars,” to be consistent with other popular rating systems that exist. The ratings for each of the components for a given satellite were averaged, and then all of the ratings for each of the satellites for a given run were averaged to give an overall star rating for each of the 662 simulations.

From these star ratings, a few conclusions can be made:

1. When evaluating individual models, the difference between RMS and nRMS error does not appear to matter much, since the star ratings for each model, when compared to other models, are very similar. When exploring how models work as a function of activity level, the normalized RMS reduces some of the dependence on activity, since both the errors and the background levels are larger during active time periods.
2. Runs with higher activity, as quantified by the Dst index, tend to have worse star ratings. This is especially true in the data-model comparisons in the inner magnetosphere, indicating that the ring current dynamics may play a role in this. This finding is similar to the finding of *Rastätter et al.* [2013], who showed that coupling an MHD code to ring current model provided better results when compared to Dst during a storm. Satellites that were not in the inner magnetosphere tended to have higher ratings during active time periods.
3. There is a clear bias in the B_z component of the geosynchronous magnetic field simulation results, indicating that the models do not have strong enough stretching of the dipole. This bias was not observed in nongeosynchronous satellites.
4. The best model, as determined by the star ratings, was BATSRUS coupled to the RCM, which indicates that the presence of an inner magnetosphere model improves the model's ability to accurately reproduce the magnetic field in the magnetosphere. When the inner magnetospheric model was not included (i.e., going from BATSRUS with the RCM to BATSRUS alone), the star rating decreased by 0.10–0.15 stars.
5. Most of the models' distributions of star ratings are statistically different from each other, indicating that the models definitely have strengths and weaknesses that are unique, although GUMICS did not really have enough model runs to statistically differentiate it from other models.

Acknowledgments

All data for this study are available through the Community Coordinated Modeling Center website (<http://ccmc.gsfc.nasa.gov/>) and the Virtual Model Repository website (<http://vmr.engin.umich.edu/>). This study would not have been possible without the Community Coordinated Modeling Center, which is funded by the National Science Foundation, National Aeronautical and Space Administration, the Air Force Office of Scientific Research, and others. At the University of Michigan, the research was funded by NASA grant NNX12AQ40G. Special thanks go to Casey Steuer, Nicholas Perlongo, Jie Zhu, Xiangyun Zhang, Charles Bussy-Virat, and Nathan Boll, who helped edit this paper.

References

- De Zeeuw, D. L., S. Sazykin, R. A. Wolf, T. I. Gombosi, A. J. Ridley, and G. Tóth (2004), Coupling of a global MHD code and an inner magnetospheric model: Initial results, *J. Geophys. Res.*, *109*, A12219, doi:10.1029/2003JA010366.
- Fedder, J., and J. Lyon (1987), The solar wind–magnetosphere–ionosphere current–voltage relationship, *Geophys. Res. Lett.*, *14*, 880–883.
- Fedder, J., S. Slinker, and J. Lyon (1998), A comparison of global numerical simulation to data for the January 27–28, 1992, geospace environment modeling challenge event, *J. Geophys. Res.*, *103*, 14,799–14,810.
- Fok, M.-C., R. B. Horne, N. P. Meredith, and S. A. Glauert (2008), Radiation belt environment model: Application to space weather nowcasting, *J. Geophys. Res.*, *113*, A03S08, doi:10.1029/2007JA012558.
- Fuller-Rowell, T., and D. Rees (1983), Derivation of a conservative equation for mean molecular weight for a two-constituent gas within a three-dimensional, time-dependent model of the thermosphere, *Planet. Space Sci.*, *31*, 1209–1222.
- Glocer, A., G. Toth, M. Fok, T. Gombosi, and M. Liemohn (2009), Integration of the radiation belt environment model into the space weather modeling framework, *J. Atmos. Sol. Terr. Phys.*, *71*, 1653–1663, doi:10.1016/j.jastp.2009.01.003.
- Gombosi, T., et al. (2004), Solution adaptive MHD for space plasmas: Sun-to-Earth simulations, *Comput. Sci. Eng.*, *6*, 14–35.
- Gombosi, T. I., G. Tóth, D. L. De Zeeuw, K. C. Hansen, K. Kabin, and K. G. Powell (2001), Semi-relativistic magnetohydrodynamics and physics-based convergence acceleration, *J. Comput. Phys.*, *177*, 176–205.
- Gordeev, E., V. Sergeev, I. Honkonen, M. Kuznetsova, L. Rastätter, M. Palmroth, P. Janhunen, G. Tóth, J. Lyon, and M. Wiltberger (2015), Assessing the performance of community-available global MHD models using key system parameters and empirical relationships, *Space Weather*, *13*, 868–884, doi:10.1002/2015SW001307.
- Honkonen, I., L. Rastätter, A. Grocott, A. Pulkkinen, M. Palmroth, J. Raeder, A. J. Ridley, and M. Wiltberger (2013), On the performance of global magnetohydrodynamic models in the Earth's magnetosphere, *Space Weather*, *11*, 313–326, doi:10.1002/swe.20055.

- Janhunen, P. (1996), GUMICS-3: A global ionosphere-magnetosphere coupling simulation with high ionospheric resolution, in *Proceedings of the ESA 1996 Symposium on Environment Modelling for Space-Based Applications, ESA SP-392*, edited by W. Burke and T.-D. Guyenne, pp. 233–239, ESA, Noordwijk, Netherlands.
- Kleiber, W., B. Hendershott, S. R. Sain, and M. Wiltberger (2016), Feature-based validation of the Lyon-Fedder-Mobarry magnetohydrodynamical model, *J. Geophys. Res. Space Physics*, *121*, 1192–1200, doi:10.1002/2015JA021825.
- Korth, H., L. Rastätter, B. J. Anderson, and A. J. Ridley (2011), Comparison of the observed dependence of large-scale Birkeland currents on solar wind parameters with that obtained from global simulations, *Ann. Geophys.*, *29*(10), 1809–1826, doi:10.5194/angeo-29-1809-2011.
- Lyon, J., J. Fedder, and C. Mobarry (2004), The Lyon-Fedder-Mobarry (LFM) global MHD magnetospheric simulation code, *J. Atmos. Sol. Terr. Phys.*, *66*, 1333–1350, doi:10.1016/j.jastp.2004.03.020.
- Merkin, V., and J. Lyon (2010), Effects of the low-latitude ionospheric boundary condition on the global magnetosphere, *J. Geophys. Res.*, *115*, A10202, doi:10.1029/2010JA015461.
- Palmroth, M., P. Janhunen, T. Pulkkinen, and W. Peterson (2001), Cusp and magnetopause locations in global MHD simulation, *J. Geophys. Res.*, *106*, 29,435–29,450, doi:10.1029/2001JA900132.
- Palmroth, M., P. Janhunen, T. I. Pulkkinen, and H. E. J. Koskinen (2004), Ionospheric energy input as a function of solar wind parameters: Global MHD simulation results, *Ann. Geophys.*, *22*, 549–566, doi:10.5194/angeo-22-549-2004.
- Palmroth, M., P. Janhunen, T. I. Pulkkinen, A. Aksnes, G. Lu, N. Ostgaard, J. Watermann, G. D. Reeves, and G. A. Germany (2005), Assessment of ionospheric Joule heating by GUMICS-4 MHD simulation, AMIE, and satellite-based statistics: Towards a synthesis, *Ann. Geophys.*, *23*, 2051–2068, doi:10.5194/angeo-23-2051-2005.
- Palmroth, M., P. Janhunen, G. A. Germany, D. Lummerzheim, K. Liou, D. N. Baker, C. Barth, A. T. Weatherwax, and J. Watermann (2006), Precipitation and total power consumption in the ionosphere: Global MHD simulation results compared with Polar and SNOE observations, *Ann. Geophys.*, *24*, 861–872, doi:10.5194/angeo-24-861-2006.
- Powell, K., P. Roe, T. Linde, T. Gombosi, and D. L. De Zeeuw (1999), A solution-adaptive upwind scheme for ideal magnetohydrodynamics, *J. Comput. Phys.*, *154*, 284–309.
- Pulkkinen, A., L. Rastätter, M. Kuznetsova, M. Hesse, A. Ridley, J. Raeder, H. J. Singer, and A. Chulaki (2010), Systematic evaluation of ground and geostationary magnetic field predictions generated by global magnetohydrodynamic models, *J. Geophys. Res.*, *115*, A03206, doi:10.1029/2009JA014537.
- Pulkkinen, A., et al. (2011), Geospace environment modeling 2008–2009 challenge: Ground magnetic field perturbations, *Space Weather*, *9*, S02004, doi:10.1029/2010SW000600.
- Raeder, J. (2003), Global magnetohydrodynamics—A tutorial, in *Space Plasma Simulation, Lect. Notes Phys.*, vol. 615, edited by J. Büchner, C. Dum, and M. Scholer, pp. 212–246, Springer, Berlin.
- Raeder, J., J. Berchem, and M. Ashour-Abdalla (1996), The importance of small scale processes in global MHD simulations: Some numerical experiments, in *The Physics of Space Plasmas*, vol. 14, edited by T. Chang and J. R. Jasperse, p. 403, MIT Center for Theor. Geo/Cosmo Plasma Phys., Cambridge, Mass.
- Raeder, J., J. Berchem, M. Ashour-Abdalla, L. Frank, W. Paterson, K. Ackerson, S. Kokubun, T. Yamamoto, and J. Slavin (1997), Boundary layer formation in the magnetotail: Geotail observations and comparisons with a global MHD simulation, *Geophys. Res. Lett.*, *24*, 951–954.
- Raeder, J., J. Berchem, and M. Ashour-Abdalla (1998), The geospace environment modeling grand challenge: Results from a global geospace circulation model, *J. Geophys. Res.*, *103*, 14,787–14,798, doi:10.1029/98JA00014.
- Raeder, J., R. McPherron, L. Frank, S. Kokubun, G. Lu, T. Mukai, W. Paterson, J. Sigwarth, H. Singer, and J. Slavin (2001a), Global simulation of the geospace environment modeling substorm challenge event, *J. Geophys. Res.*, *106*, 381–395, doi:10.1029/2000JA000605.
- Raeder, J., Y. Wang, and T. Fuller-Rowell (2001b), Geomagnetic storm simulation with a coupled magnetosphere-ionosphere-thermosphere model, in *Space Weather, Geophys. Monogr. Ser.*, vol. 125, edited by P. Song, H. Singer, and G. Siscoe, pp. 377–384, AGU, Washington, D. C.
- Rastätter, L., M. M. Kuznetsova, A. Vapirev, A. Ridley, M. Wiltberger, A. Pulkkinen, M. Hesse, and H. J. Singer (2011), Geospace environment modeling 2008–2009 challenge: Geosynchronous magnetic field, *Space Weather*, *9*, S04005, doi:10.1029/2010SW000617.
- Rastätter, L., et al. (2013), Geospace environment modeling 2008–2009 challenge: *Dst* index, *Space Weather*, *11*, 187–205, doi:10.1002/swe.20036.
- Rastätter, L., et al. (2016), GEM-CEDAR challenge: Poynting flux at DMSP and modeled Joule heat, *Space Weather*, *14*, 113–135, doi:10.1002/2015SW001238.
- Ridley, A., and M. Liemohn (2002), A model-derived stormtime asymmetric ring current driven electric field description, *J. Geophys. Res.*, *107*(A8), 1290, doi:10.1029/2001JA000051.
- Ridley, A., K. Hansen, G. Tóth, D. L. De Zeeuw, T. Gombosi, and K. Powell (2002), University of Michigan MHD results of the GGCM metrics challenge, *J. Geophys. Res.*, *107*(A10), 1290, doi:10.1029/2001JA000253.
- Ridley, A., T. Gombosi, and D. L. De Zeeuw (2004), Ionospheric control of the magnetospheric configuration: Conductance, *Ann. Geophys.*, *22*, 567–584.
- Ridley, A. J., D. L. De Zeeuw, T. I. Gombosi, and K. G. Powell (2001), Using steady state MHD results to predict the global state of the magnetosphere-ionosphere system, *J. Geophys. Res.*, *106*, 30,067–30,076.
- Ridley, A. J., T. I. Gombosi, I. V. Sokolov, G. Tóth, and D. T. Welling (2010), Numerical considerations in simulating the global magnetosphere, *Ann. Geophys.*, *28*, 1589–1614, doi:10.5194/angeo-28-1589-2010.
- Stout, Q. F., D. L. De Zeeuw, T. I. Gombosi, C. P. T. Groth, H. G. Marshall, and K. G. Powell (1997), Adaptive blocks: A high-performance data structure, paper presented at 1997 ACM/IEEE conference on Supercomputing, ACM, New York.
- Taktakishvili, A., M. Kuznetsova, M. Hesse, L. Rastätter, A. Chulaki, and A. Pulkkinen (2007), Metrics analysis of the coupled Block Adaptive-Tree Solar Wind Roe-Type Upwind Scheme and Fok ring current model performance, *Space Weather*, *5*, S11004, doi:10.1029/2007SW000321.
- Tanaka, T. (1995), Generation mechanisms for magnetosphere-ionosphere current systems deduced from a three-dimensional MHD simulation of the solar wind-magnetosphere-ionosphere coupling processes, *J. Geophys. Res.*, *100*, 12,057–12,074, doi:10.1029/95JA00419.
- Toffoletto, F., S. Sazykin, R. Spiro, R. Wolf, and J. Lyon (2004), RCM meets LFM: Initial results of one-way coupling, *J. Atmos. Sol. Terr. Phys.*, *66*, 1361–1370, doi:10.1016/j.jastp.2004.03.022.
- Tóth, G., et al. (2005), Space weather modeling framework: A new tool for the space science community, *J. Geophys. Res.*, *110*, A12226, doi:10.1029/2005JA011126.
- Wang, W., M. Wiltberger, A. Burns, S. Solomon, T. Killeen, N. Maruyama, and J. Lyon (2004), Initial results from the coupled magnetosphere–ionosphere–thermosphere model: Thermosphere–ionospheric responses, *J. Atmos. Sol. Terr. Phys.*, *66*, 1425–1441, doi:10.1016/j.jastp.2004.04.008.

- Wang, H., A. Ridley, and H. Lühr (2008), Validation of the space weather modeling framework using observations from CHAMP and DMSP, *Space Weather*, *6*, S03001, doi:10.1029/2007SW000355.
- Welling, D., and M. Liemohn (2014), Outflow in global magnetohydrodynamics as a function of a passive inner boundary source, *J. Geophys. Res. Space Physics*, *119*, 2691–2705, doi:10.1002/2013JA019374.
- Welling, D., and A. Ridley (2010a), Validation of SWMF magnetic field and plasma, *Space Weather*, *8*, S03002, doi:10.1029/2009SW000494.
- Welling, D., and S. Zaharia (2012), Ionospheric outflow and cross polar cap potential: What is the role of magnetospheric inflation?, *Geophys. Res. Lett.*, *39*, L23101, doi:10.1029/2012GL054228.
- Welling, D., V. Jordanova, S. Zaharia, A. Gloer, and G. Toth (2011), The effects of dynamic ionospheric outflow on the ring current, *J. Geophys. Res.*, *116*, A00J19, doi:10.1029/2010JA015642.
- Welling, D. T., and A. J. Ridley (2010b), Exploring sources of magnetospheric plasma using multispecies MHD, *J. Geophys. Res.*, *115*, A04201, doi:10.1029/2009JA014596.
- White, W. W., G. L. Siscoe, G. M. Erickson, Z. Kaymaz, N. C. Maynard, K. D. Siebert, B. U. Ö. Sonnerup, and D. R. Weimer (1998), The magnetospheric sash and the cross-tail S, *Geophys. Res. Lett.*, *25*, 1605–1608.
- Wiltberger, M., W. Wang, A. Burns, S. Solomon, J. Lyon, and C. Goodrich (2004), Initial results from the coupled magnetosphere ionosphere thermosphere model: Magnetospheric and ionospheric response, *J. Atmos. Sol. Terr. Phys.*, *66*, 1411–1423, doi:10.1016/j.jastp.2004.03.026.
- Winglee, R. (1995), Regional particle simulations and global two-fluid modelling of the magnetospheric current system, in *Cross-Scale Coupling in Space Plasmas*, *Geophys. Mongr. Ser.*, vol. 93, edited by R. Winglee, pp. 71–80, AGU, Washington, D. C.
- Winglee, R. (1998), Multi-fluid simulations of the magnetosphere: The identification of the geopause and its variation with IMF, *Geophys. Res. Lett.*, *25*, 4441–4444.
- Yu, Y., and A. Ridley (2008), Validation of the space weather modeling framework using ground-based magnetometers, *Space Weather*, *6*, S05002, doi:10.1029/2007SW000345.
- Yu, Y., and A. Ridley (2013a), Exploring the influence of ionospheric O⁺ outflow on magnetospheric dynamics: The effect of outflow intensity, *J. Geophys. Res. Space Physics*, *118*, 5522–5531, doi:10.1002/jgra.50528.
- Yu, Y., and A. Ridley (2013b), Exploring the influence of ionospheric O⁺ outflow on magnetospheric dynamics: Dependence on the source location, *J. Geophys. Res. Space Physics*, *118*, 1711–1722, doi:10.1029/2012JA018411.
- Yu, Y., A. Ridley, D. Welling, and G. Tóth (2010), Including gap-region field-aligned currents and magnetospheric currents in the MHD calculation of ground-based magnetic field perturbations, *J. Geophys. Res.*, *115*, A08207, doi:10.1029/2009JA014869.
- Zaharia, S., V. K. Jordanova, D. Welling, and G. Tóth (2010), Self-consistent inner magnetosphere simulation driven by a global MHD model, *J. Geophys. Res.*, *115*, A12228, doi:10.1029/2010JA015915.
- Zhang, B., W. Lotko, M. J. Wiltberger, O. J. Brambles, and P. A. Damiano (2011), A statistical study of magnetosphere-ionosphere coupling in the Lyon-Fedder-Mobarry global MHD model, *J. Atmos. Sol. Terr. Phys.*, *73*, 686–702, doi:10.1016/j.jastp.2010.09.027.
- Zhang, J., et al. (2007), Understanding storm-time ring current development through data-model comparisons of a moderate storm, *J. Geophys. Res.*, *112*, A04208, doi:10.1029/2006JA011846.